New Journal of Physics
The open access journal at the forefront of physics
Deutsche Physikalische Gesellschaft DPG | IOP Institute of Physics

Universally optimal noisy quantum walks on complex networks

Filippo Caruso
LENS and Dipartimento di Fisica e Astronomia, Università di Firenze, I-50019 Sesto Fiorentino, Italy and
QSTAR, Largo Enrico Fermi 2, I-50125 Firenze, Italy
E-mail: filippo.caruso@lens.unifi.it

Received 6 December 2013, revised 4 March 2014
Accepted for publication 20 March 2014
Published 28 May 2014
New Journal of Physics **16** (2014) 055015
doi:10.1088/1367-2630/16/5/055015

Abstract
Transport properties play a crucial role in several fields of science, for example biology, chemistry, sociology, information science and physics. The behavior of many dynamical processes running over complex networks is known to be closely related to the geometry of the underlying topology, but this connection becomes even harder to understand when quantum effects come into play. Here, we exploit the Kossakowski–Lindblad formalism of quantum stochastic walks to investigate the capability of quickly and robustly transmitting energy (or information) between two distant points in very large complex structures, remarkably assisted by external noise and quantum features such as coherence. An optimal mixing of classical and quantum transport is, very surprisingly, quite universal for a large class of complex networks. This widespread behavior turns out to be also extremely robust with respect to geometry changes. These results might pave the way for designing optimal bio-inspired geometries of efficient transport nanostructures that can be used for solar energy and also quantum information and communication technologies.

Keywords: quantum transport, transfer efficiency, complex networks

1. Introduction

The static properties and dynamical performances of complex network structures have been extensively studied in classical statistical physics [1]. In the past few years there has been a growing interest in fully understanding how these studies can be generalized when dealing with quantum mechanical systems, e.g. with microscopic and fragile quantum coherence affecting macroscopic and robust transport behavior.

Very recently, it has been found that quantum effects play a crucial role in the remarkably efficient energy transport phenomena in light-harvesting complexes [2–8], also with a fundamental contribution of the external noisy environment [9–13]. Indeed, an electronic exciton seems to behave as a quantum walker over these protein structures, exploiting quantum superposition and interference to enhance its capability to travel from an antenna complex, where light is absorbed, to the reaction center, where this energy is converted into a more available chemical form. More generally, quantum walks [14] are becoming more and more popular recently, since they have potential applications not only in energy transport [15], but also in, for instance, quantum information theory [16–22] since they may lead to quantum algorithms with polynomial as well as exponential speedups [23], e.g. the Grover search algorithm [24], universal models for quantum computation [25], state transfer in spin and harmonic networks [26–29], noise-assisted quantum communication [29], and also very recent proposals for Google page ranking [30–33]. The generalization of classical random walks into the quantum domains had led to different variants, mainly discrete-time quantum walks [14], based on an additional action of a quantum 'coin', and continuous-time quantum walks obtained, basically, by mapping the classical transfer matrix into a system Hamiltonian [17]; notice, however, that these two kinds of walks are shown to be connected by a precise limiting procedure [34].

On top of that, this growing interest has been especially stimulated by the increasing number of fascinating and challenging experiments demonstrating the basic features of quantum walks. They have been implemented, for instance, with NMR [35, 36], trapped ions [37, 38], neutral atoms [39], and several photonic schemes such as waveguide structures [40], bulk optics [41, 42], fiber loop configurations [43–45], and miniaturized integrated waveguide circuits [46–48]. Most of these experiments included a single walker moving on a line, and only very recently have they implemented optical quantum walks on a square lattice by laser pulses [44] and single photons [45]. Experiments with two walkers on a line have been reported in [46–48], motivated also by the fact that the introduction of multiple walkers allows one to map a quantum walk on a line into higher dimensional lattices [49].

Therefore, given these first experimental attempts at higher dimensional quantum walks, it turns out to be timely and interesting to investigate in more detail the transport features of quantum walkers over large complex networks. Furthermore, motivated by our previous results on noise-enhanced transfer of energy and information over light-harvesting complexes and communication networks [12, 29], we consider it worth pursuing a deeper understanding of the additional mixing of quantum features with classical transport behavior when varying the underlying (high dimensional) network topology. A recent study on the comparison of quantum energy transfer and classical energy transfer, by noisy cellular automata, can be found in [50]. Fractal geometries have also been exploited in studying the role of the topological structure in quantum transport [51] and for Grover-based searching problems [52]—for a review on continuous-time quantum walks on complex networks see also [15]. As regards the role of

decoherence in the mixing time of both discrete-time and continuous-time quantum walks, especially for chains, cycles and hypercubes, a review appears in [21]. Moreover, in the context of light-harvesting phenomena, the role of geometry has also been investigated in terms of structure optimization [53], in the presence of disordered systems [54, 55], and to propose design principles for biomimetic structures [56].

The outline of the paper is the following. In section 2.1 we recall the standard formalism of complex networks, that are completely defined by their so-called adjacency matrices and spectral properties [57]. In particular, one can define statistical measures of distances between nodes in terms of shortest path lengths and the corresponding maximum (or graph diameter), and local properties such as the clustering coefficient measuring the connectivity of each vertex. In section 2.2, we describe the Kossakowski–Lindblad formalism of quantum stochastic walks, in terms of well-defined master equations, generalizing classical (random) and quantum walks by including all possible transition elements from a vertex as given by the connectivity of the graph (adjacency matrix) [58]. This formalism includes also, as a special case, a model showing both classical and quantum walk behaviors as extreme cases and the classical–quantum transition in the other regimes. Our figure of merit for the transport efficiency of each graph is also defined. After these introductory sections, we investigate this model for a family of large complex networks, comparing the corresponding transport performances—see section 3. In particular, we find that the same mixing of classical and quantum behaviors leads to the optimal transfer efficiency for all graphs studied. This widespread behavior is shown to be very robust when one modifies or deletes some links of the structure. Finally, some conclusions and the outlook are discussed in section 4.

2. The model

Here we briefly introduce the main notions of complex networks, together with some well-defined geometric measures, and then the formalism of quantum stochastic walks that has been considered in this paper in order to implement the transport dynamics over these graphs.

2.1. Network topology: definitions and measures

The structure of a complex network or graph G can be described by a pair $G = \left(V, E\right)$, with $V(G)$ being a non-empty and finite set whose elements are called vertices (or nodes) and $E(G)$ being a non-empty set of unordered pairs of vertices, called edges (or links). Let us denote with N the number of nodes of the graph G, i.e. the number of elements in $V(G)$, and with L the number of links or elements of $E(G)$. A graph is completely defined by its adjacency matrix A as follows:

$$\left[A\right]_{i,j} := \begin{cases} 1 & \text{if} \left\{ V_i, V_j \right\} \in \text{E(G)} \\ 0 & \text{if} \left\{ V_i, V_j \right\} \notin \text{E(G)}. \end{cases} \tag{1}$$

Moreover, if $\left\{ V_i, V_j \right\} \in E(G)$, the vertices V_i and V_j are said to be adjacent or neighboring. The number of adjacent vertices or neighbors of the vertex V_i is denoted as d_i and is called the degree (or connectivity) of V_i, i.e. $d_i = \sum_{j=1}^{N} A_{ij}$. Notice that a graph is said to be regular if each of its

nodes has the same degree, i.e. $d_i = d$ for any i. In the following, we will consider only connected graphs, where there is always a path connecting any two nodes, since the unconnected subgraphs or isolated vertices do not play any role in the transport dynamics occurring over the rest of the network. Moreover, we restrict our consideration to graphs without loops, i.e. without edges of the form $\{V_i, V_i\}$, i.e. $A_{ii} = 0$ for any i.

Although there are several measures of network topology in the literature [1], here we focus on the ones that are more related to our study. First of all, the number of hops from the node i to j with length k equals A_{ij}^k. Then, the shortest path length $\mathcal{L}_{ij}$ between i and j is the minimum number of steps (geodesic lengths) for going from node i to node j, i.e.

$$\mathcal{L}_{ij} = \min k: \ A_{ij}^k > 0 \text{ while } A_{ij}^m = 0 \text{ for } m < k \ . \tag{2}$$

The so-called characteristic path length $\mathcal{L}$ is hence defined as the average of the shortest paths between all possible pairs of nodes, i.e. $\mathcal{L} = \left(1/\bar{L}\right)\sum_{ij}\mathcal{L}_{ij}$ with $\bar{L} = N\left(N-1\right)/2$ being the total number of node pairs. Furthermore, the largest $\mathcal{L}_{ij}$ is defined as the diameter D of the graph, that is the largest distance (or longest shortest path) between any two vertices of a graph. It corresponds also to the lowest integer k for which $\left(A^k\right)_{ij} \neq 0$ and $\left(A^m\right)_{ij} = 0$ if $m < k$ for each couple of nodes i and j, i.e.

$$D = \max_{i,j}\mathcal{L}_{ij}. \tag{3}$$

Note that for any graph, $1 \leqslant D \leqslant N-1$. Furthermore this quantity is closely related to the spectral properties of A. A well-known theorem in the spectral theory of complex networks states, in fact, that the number of distinct eigenvalues π of the adjacency matrix A is at least equal to $D+1$, i.e. $\pi \geqslant D+1$ [57]. On one hand, the network with the smallest diameter is the complete or fully connected (FC) graph, where one has $D = 1$, since all pairs of nodes are connected through a link. Indeed, the latter is the only graph whose adjacency matrix A has only two different eigenvalues ($N-1$ with degeneracy 1 and -1 with degeneracy $N-1$; note that the trace of A, and thus the sum of its eigenvalues, has to always be 0) and the bound above between D and π is tight. On the other hand, for a given number of vertices N, the linear chain is the topology with the largest diameter ($D = N-1$).

Finally, another measure of the graph connectivity, known as the clustering coefficient C, quantifies how well the neighborhood of a node is connected [59]. Given a node i, let us define G_i as its neighborhood, i.e. the graph represented by the set of neighbors of the vertex i and the relative interconnecting links. Then C_i is the local clustering coefficient of the node i and is defined as $C_i = 2e_i/\left(d_i\left(d_i-1\right)\right)$, with e_i being the number of links in G_i and d_i the degree of the node i, i.e. it is the ratio of the number of links in G_i (e_i) over its maximum possible number $\left(d_i\left(d_i-1\right)/2\right)$. The (global) cluster coefficient C of the graph G is then given by the average of C_i over all sites i, i.e.,

$$C = \frac{1}{N}\sum_{i=1}^{N}\frac{2e_i}{d_i\left(d_i-1\right)} \ , \tag{4}$$

and it is always in the range $\left[0, 1\right]$.

2.2. Transport dynamics: quantum stochastic walks

Once we have introduced the topological structure of our model, we need to specify the corresponding dynamics. To start with, let us recall that a random walk is usually defined as a time-discrete process where at each step the walker jumps between two connected nodes of the graph G with some probability described by the transition matrix $T = \left\{T_{ij}\right\}$ [60]. Usually, one has $T_{ij} = A_{ij}/d_i$ for classical random walks, which is indeed called the random walk normalized Laplacian matrix. More specifically, the Laplacian matrix L is $L = A - D$, where D is the diagonal matrix of the vertex degrees, i.e. $D = \left\{d_i\right\}$, while $T = D^{-1}A$. Given the occupation probability distribution $\vec{q}_t \equiv \left\{q_i^{(t)}\right\}$ of the walker over the nodes V_i at a time t, the distribution at time $t + 1$ is simply given by $\vec{q}_{t+1} = T\vec{q}_t$. The time-continuum version of such classical random walk (CRW) dynamics is then

$$\frac{\mathrm{d}}{\mathrm{d}t}\vec{q} = \left(T - 1\right)\vec{q}\ . \tag{5}$$

In both cases, the system ends up with a stationary (unique) distribution $\bar{q}_i = d_i/\left(2N\right)$, that is the left-eigenvector of T associated with the eigenvalue equal to 1. The rate of convergence towards the steady state $\bar{q}$, also known as the mixing rate τ_{mix}, is proportional to the so-called spectral gap of the graph G, that is the difference between the absolute values of the two largest eigenvalues of A (λ_1, λ_2), i.e. $\tau_{mix} \propto \left(\lambda_1 - \lambda_2\right)$ [57]. In other words, the larger the spectral gap is, the faster the walker converges to $\bar{q}$. Note that one always has $\lambda_1 - \lambda_2 \leqslant N$ and the bound is achieved for the FC graph. It is well known that well-connected graphs have small diameters and large spectral gaps, implying that the mixing rate τ_{mix} is larger (fast classical random walks) for graphs with larger D. There do exist several bounds showing that the mixing rate τ_{mix} monotonically increases with D, apart from some constants.

In order to study the transport properties of such networks including also quantum coherence effects, we use the general framework of continuous-time quantum stochastic walks (QSW) [58], based on the Kossakowski–Lindblad master equation, allowing us to interpolate between classical random walks (CRW) and quantum walks (QW) [20]. More specifically, the evolution of our initial state, represented by the density operator ρ, is as follows:

$$\frac{\mathrm{d}\rho}{\mathrm{d}t} = -\left(1 - p\right)\mathrm{i}\left[H, \rho\right] + p\sum_{ij}\left(L_{ij}\rho L_{ij}^{\dagger} - \frac{1}{2}\left\{L_{ij}^{\dagger}L_{ij}, \rho\right\}\right), \tag{6}$$

where H is the Hamiltonian describing the quantum coherent dynamics, while the operators L_{ij} are responsible for the irreversibility. Note the parameter $p \in \left[0, 1\right]$ quantifying the interplay between coherent (unitary) dynamics and incoherent (irreversible) dynamics. In order to match with the limit of usual CRWs on choosing $p = 1$, we assume that $L_{ij} = T_{ij}\left|\, i\right\rangle\left\langle j\,\right|$ with $\left|\, i\right\rangle$ being the site basis, recovering equation (5) for the diagonal elements of ρ, i.e. $\vec{q}_t \equiv \left\{\rho_{ii}\left(t\right)\right\}$. On the other hand, $p = 0$ corresponds to the pure QW master equation, where we choose $H = A$.

This corresponds to a simplified model of a system (for instance, a light-harvesting complex), where all the energies and couplings are the same (homogeneous graphs)[1]. For simplicity, we neglect the presence of losses and we restrict consideration to the case where only one excitation is present in the network. Note that this formalism has also been used in a different context to propose a more efficient quantum navigation algorithm for ranking elements of large (Google page) networks [30, 31]. To study the transfer efficiency of the QSW over the complex network G, on the right-hand side of equation (6) we add another Lindblad term $L_{N+1} = \Gamma \left[2|N+1\rangle\langle N| \rho |N\rangle\langle N+1| - \{|N\rangle\langle N|, \rho\} \right]$, with Γ being the irreversible rate of transfer from the site N of the graph to some external node $N+1$ (trapping site or sink) where the energy is continuously and irreversibly stored. Hence, the transfer efficiency of the graph will be measured by [10, 12, 13, 29]

$$\mathcal{E}(p, t) = 2\Gamma \int_0^t \rho_{NN}(p, t')\, \mathrm{d}t' \ . \tag{7}$$

Hence, our figure of merit will be

$$\mathcal{E}(p) \equiv \mathcal{E}(p, \bar{t}) \ \text{ with } \bar{t}\text{: } \exists\, \bar{p} \in [0, 1] \ \text{ with } \mathcal{E}(\bar{p}, \bar{t}) \simeq 1 \ , \tag{8}$$

usually corresponding to taking $\bar{t} \gg N \left|\left|A_{ij}\right|\right|^{-1}$, with $\left|\left|A_{ij}\right|\right|$ being the strength of the coupling rates, i.e. considering the trapping site population after the initial transient behavior.

3. Results

In the following we will investigate the model described above for a large class of complex networks, including up to thousands of nodes, comparing the relative transfer efficiencies $\mathcal{E}(p)$.

3.1. Regular graphs: chains and square lattices

The simplest geometry, to start with, is represented by a linear chain connecting node 1 to node N that is linked to the sink ($D = N - 1$). As shown in figure 1, when the excitation initially is on site 1 and in the absence of disorder (homogeneous chain), the quantum limit ($p = 0$) provides the optimal transport efficiency, in agreement with results obtained previously in [10, 12]. However, this is not the case when the initial site is not located opposite to the sink [61]. Indeed, if it is on the center site of the chain, the efficiency becomes optimal at the value of $p \sim 0.1$. This holds also when we average $\mathcal{E}(p)$ over all possible initial sites—see figure 1 for a chain with $N = 35$. The same optimal value is also found for longer chains, although the scaling of $\mathcal{E}(p, \bar{t})$ with N (at time $\bar{t}$, linearly proportional to N) depends on p and shows a stronger dependence on N (i.e. less robustness) in the classical limit—see the inset of figure 1.

An $m \times m$ regular square lattice is a grid graph whose $N = m^2$ vertices are on a square grid ($D = 2m - 2$) and are linked only by nearest neighbor edges—see figure 2. It is considered as a regular graph since each vertex has degree 4 (excluding the boundary nodes). This network is typically characterized by high values of $\mathcal{L}$ but small clustering coefficients C. As for linear

[1] A more realistic model including static disorder in both energy and coupling terms, with also specific distance-dependent couplings referred to particular physical systems, will be analyzed in a forthcoming paper.

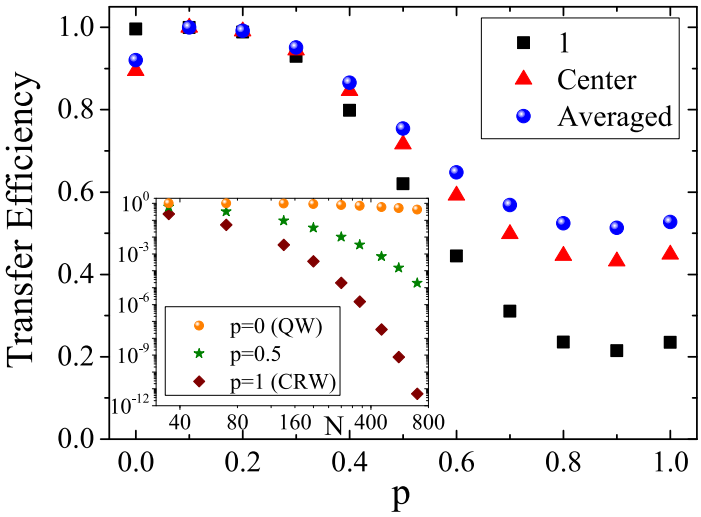

Figure 1. Transfer efficiency $\mathcal{E}(p)$ as a function of p for QSWs on a linear chain of $N = 35$ nodes. Different initial conditions are considered, while the sink is always connected to the site 35. Note that $\mathcal{E}(p)$ appears to be rising again towards $p = 1$, perhaps because the coherent dynamics tends to be frozen (the quantum Zeno effect) in presence of very strong irreversibility, but the transport is recovered again at the classical limit. However, this is not always the case for other networks—see, for instance, figure 11 for random graphs. Inset: $\mathcal{E}(p, \bar{t})$ versus N, at time $\bar{t}$, which is linearly proportional to N, in the case of a walker starting from site 1. An asymptotic power law behavior is observed but with an exponent depending on the value of p.

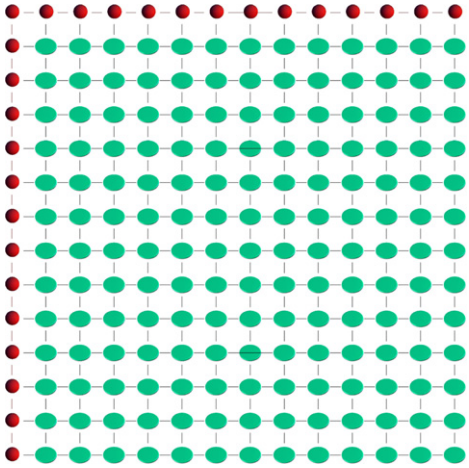

Figure 2. Square lattice of $N = 196$ nodes. The red ones represent one of the shortest paths connecting two opposite vertices, which are the injecting site (1) and the one (196) connected to the external sink.

chains, the optimal transport occurs for an intermediate mixing of quantum and classical effects, particularly for $p \sim 0.1$—see figure 3. Here and in the following, the decreasing behavior of $\mathcal{E}(p)$, for p larger than the optimal one, is intuitively expected because of quantum Zeno effects suppressing the transport dynamics.

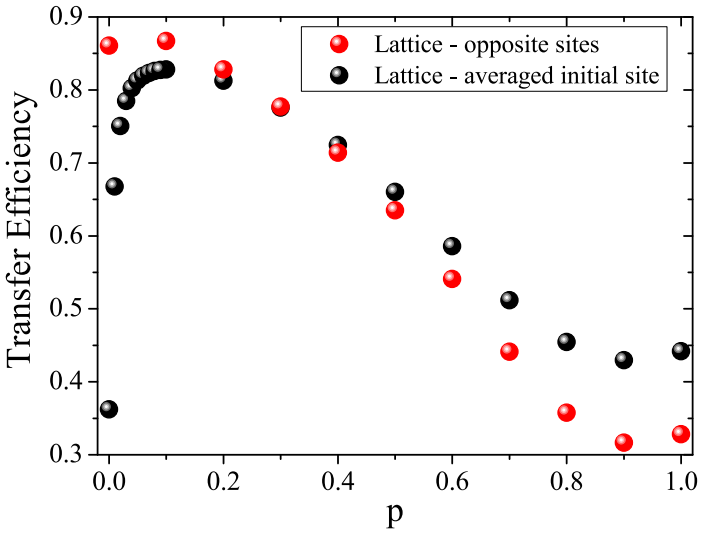

Figure 3. Transfer efficiency $\mathcal{E}(p)$ versus p for QSWs on a square lattice of $N = 196$ nodes, where the excitation is initially localized on a single site (1), while the sink is always at the site 196. The averaging over all possible initial sites is also included.

3.2. Small-world topologies

In this section, we consider another topology, known as a small-world (SW) network, that has been extensively investigated in the literature [1] as describing a plethora of realistic complex networks, ranging from the World Wide Web to protein structures. In particular, a small-world network is a graph which interpolates between a regular square lattice and a random graph (section 3.3), i.e. in which the distance between any two vertices is of the order of that for a random graph but, at the same time, the concept of neighborhood is preserved, as for regular lattices. In other words, this graph is like a square lattice with the introduction of a few long-range edges creating short-cuts between distant nodes [62]—see figure 4.

It can be constructed following the method proposed in [62], but here we follow a slightly different algorithm allowing us to keep the degree of each vertex fixed as in [63]. We start from a regular square lattice and we randomly choose a vertex V_{i_1} and the edge $V_{i_1} - V_{i_2}$ that connects vertex V_{i_1} to its nearest neighbor V_{i_2}, at random. With probability r this edge is rewired and with probability $1 - r$ it is left in place. If the edge has been rewired, (a) we choose at random a second vertex V_{j_1} and one of its edges, e.g. the edge $V_{j_1} - V_{j_2}$ connecting V_{j_1} to V_{j_2}, and (b) we replace the couple of edges $V_{i_1} - V_{i_2}$ and $V_{j_1} - V_{j_2}$ with the couple $V_{i_1} - V_{j_2}$ and $V_{j_1} - V_{i_2}$, as in the inset of figure 5. This process is repeated by moving over the entire lattice considering each vertex in turn until one lap is completed. In such a way, the limit case $r = 1$ corresponds to a random graph with fixed degree equal to 4. In the intermediate cases $0 < r < 1$ an increasing number of long-range edges turn up in the graph. In other words, the introduction of a few long-range edges creates short-cuts that connect vertices that otherwise would be much further apart. Strictly speaking, the characteristic path length $\mathcal{L}$ of the rewired graph decreases while increasing r [1]. Therefore, we can use the term 'small-world' to refer to a rewired lattice (with fixed degree) with the minimum number of rewired edges such that the characteristic path length $\mathcal{L}$ is as small as that for the corresponding random graph (with $\mathcal{L}$ depending at most

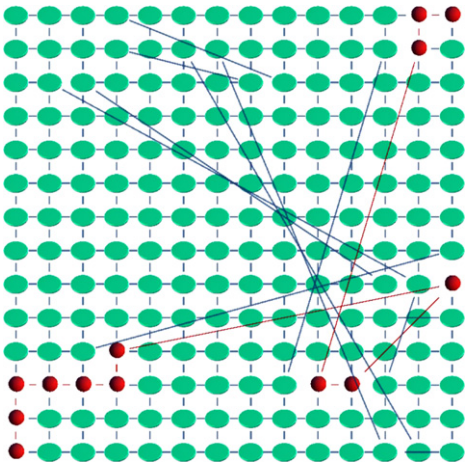

Figure 4. Small-world topology of $N = 196$ nodes. The vertices and links in red show the shortest path connecting the opposites sites of the grid where the initial excitation and sink are, respectively, located.

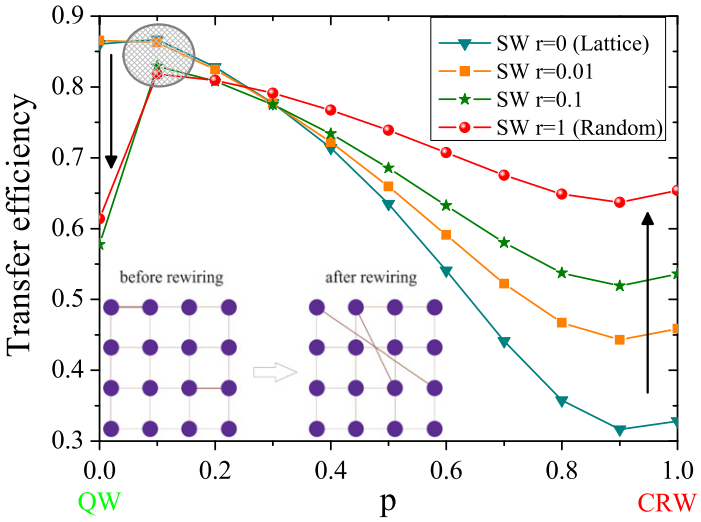

Figure 5. Transfer efficiency $\mathcal{E}(p)$ as a function of p for the case of small-world networks at different values of the rewiring probability r. The arrows are included to point out that the transfer efficiency increases (decreases) when adding long-range links for the classical (quantum) case. Inset: a schematic representation of the rewiring procedure interpolating between a regular ($r = 0$) and a random topology ($r = 1$), keeping the degree of each vertex fixed and equal to 4 [63].

logarithmically on the network size N), but the cluster coefficient C is still as high as for a regular lattice, i.e. much larger than C for random networks [62]. As shown also in [63], this is obtained already for very small values of r ($r \simeq 0.01$), well before the random graph limit ($r = 1$). Notice that this model undergoes a 'genuine' continuous phase transition as the density of short-cuts tends to zero, with a characteristic length diverging as r^{-1} [1]. Now we study the QSW dynamics over this geometry when varying the mixing p of classical and quantum behavior. Again, as shown in figure 5, we find the optimality of $p \sim 0.1$ for different

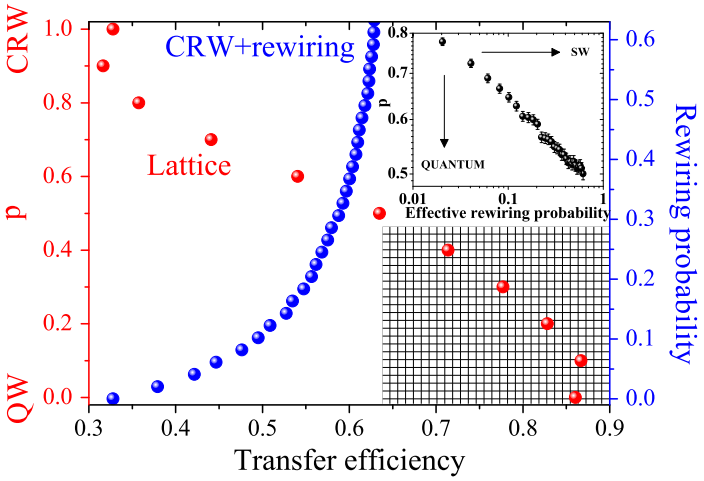

Figure 6. SW transition: QSW transfer efficiency $\mathcal{E}(p)$ when varying p for a square lattice ($r = 0$; left vertical axis, red) and when changing the rewiring probability r of a small-world network for CRW ($p = 1$; right vertical axis, blue). The grid-shadow region cannot be achieved by CRWs no matter how many long-range links are added to the graph. Inset: effective rewiring probability r_e for a CRW to reproduce the same transport efficiency as a lattice QSW with different values of p. The presence of more quantum coherence, in the square lattice QSW case, corresponds to a higher number of long-range links in the SW–CRW model, and these two quantities scale as a power law (with exponent $\simeq -0.13$).

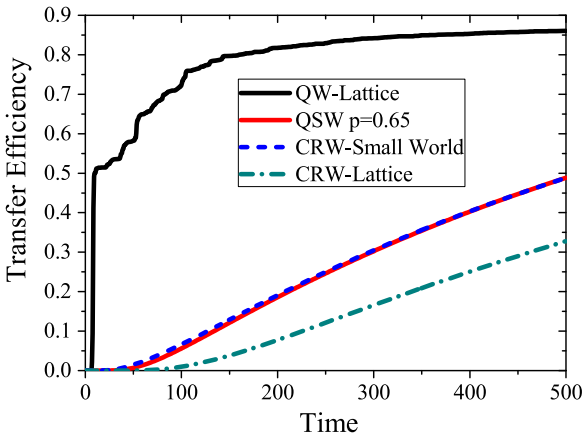

Figure 7. Comparison of $\mathcal{E}(p, t)$ time evolutions of a CRW ($p = 1$) on a SW network with $r \sim 0.09$ and a QSW on a square lattice for $p \sim 0.65$. The extreme cases of QWs ($p = 0$) and CRWs ($p = 1$) on a square lattice are also shown.

values of rewiring probabilities r. Notice that the curves in figure 5 become flatter and flatter for higher r because, in the limit of a random graph, $\mathcal{E}(p)$ is expected to weakly depend on p. See also [64] for other studies of quantum transport on small-world networks.

Furthermore, we analyze the connection, if any, between the value of p for QSWs on a square lattice and the value of r for CRWs on a rewired small-world structure (the SW–CRW case)—see figure 6. In other words, we extract the effective value of the rewiring probability r_e

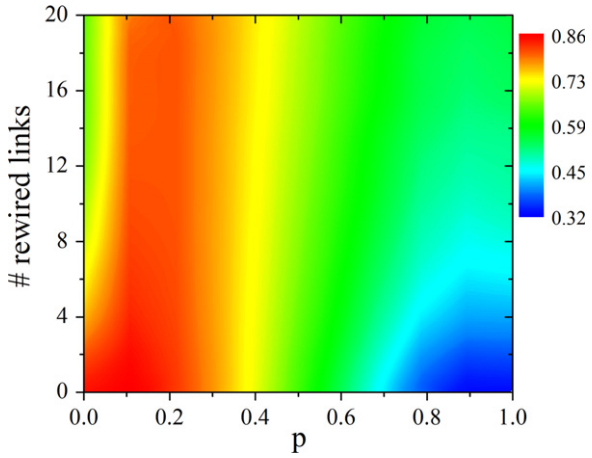

Figure 8. Behavior of the transfer efficiency $\mathcal{E}(p)$ versus the number of randomly rewired links for QSWs on a square lattice geometry of $N = 196$ nodes.

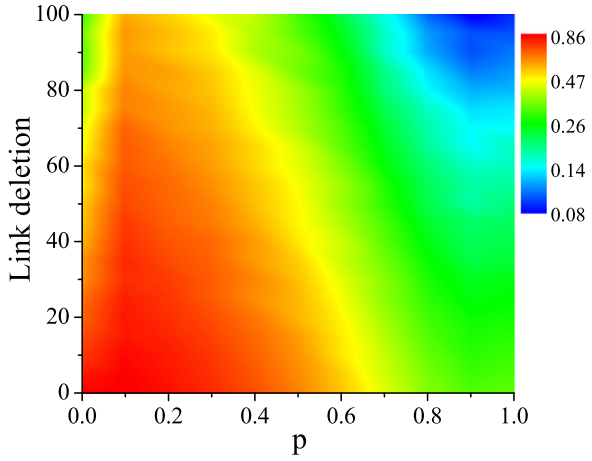

Figure 9. Behavior of the transfer efficiency $\mathcal{E}(p)$ versus the number of randomly deleted links for QSWs on a square lattice geometry of $N = 196$ nodes.

providing the same transport efficiency as corresponds to a given value of p. It turns out that these two quantities, p and r_e, are related and, in particular, follow a power law behavior (see the inset of figure 6). The more coherent the lattice QSW dynamics, the higher the number of long-range links required in the SW–CRW model in order to achieve the same energy transferred into the sink. A comparison of the corresponding time evolutions $\mathcal{E}(p, t)$ of the transfer efficiency for given values of r_e and p is shown in figure 7. Therefore, not only is $\mathcal{E}(p)$ the same in correspondence with the mapped p and with r_e, but also the full time evolutions $\mathcal{E}(p, t)$ follow the same behaviors. Besides this, let us point out that there are a range of high values of transfer efficiency obtained for small p (i.e., closer to the quantum limit), that no CRW can achieve no matter how many long-range links may be added. Examples of kinetic models of energy transport with nonlocal links were studied in [65].

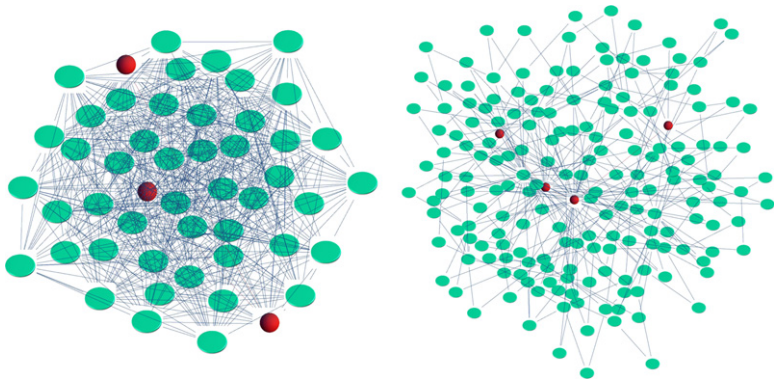

Figure 10. Examples of RG (left) and SF networks with $\gamma \sim 3$ (right). The red nodes represent a geodesic path from the vertex 1 (initial excitation) to the vertex N to which the sink is connected.

Finally, we focus on the robustness of the transport efficiency optimality with respect to rewiring or deleting links. In the context of complex network theory, this is called static robustness and usually refers to the resilience of real graphs (electric networks, WWW, social networks, etc) against external attacks or random failures [1]. As shown in figures 8 and 9, the optimality of $p \sim 0.1$ is very robust against an increasing number of rewired or deleted links. This geometric robustness is also especially relevant when one is dealing with real physical systems behaving as noisy quantum walkers on imperfect structures.

3.3. Random and scale-free graphs

Another important class of complex networks is represented by random graphs (RG) and scale-free (SF) networks [1]. RGs are defined as structures with Poissonian distribution of the node degree, and can be constructed also as limiting cases ($r \to 1$) of the small-world networks studied above—see the example in the left panel of figure 10. They are also characterized by small values of both $\mathcal{L}$ and C. A scale-free network is, in contrast, a graph with a power law degree distribution $p(d) \sim d^{-\gamma}$ of the vertex degree d. It displays a small characteristic path length $\mathcal{L}$ as for a small-world network and for a random graph, but it differs from them in having a power law degree distribution. This graph can be constructed in the following way. By using the preferential attachment growing procedure introduced by Barabási and Albert [66], one starts from $v + 1$ all-to-all connected vertices and at each time step one adds a new vertex with v edges. These r edges point to old vertices with probability $q_i = \frac{d_i}{\sum_j d_j}$, where d_i is the degree of the vertex V_i, as defined in section 2.1. This procedure allows a selection of the γ exponent of the power law degree scaling, with $\gamma = 3$ in the thermodynamic limit (i.e., $N \longrightarrow \infty$)—see the example in the right panel of figure 10.

The dependence on p of the transfer efficiency $\mathcal{E}(p)$ is shown for both graphs in figure 11. Again, but still interestingly, the transport efficiency optimality is reached for $p \sim 0.1$. Another study of continuous-time quantum walks on random graphs, but only for CRWs and QWs, is shown in [67].

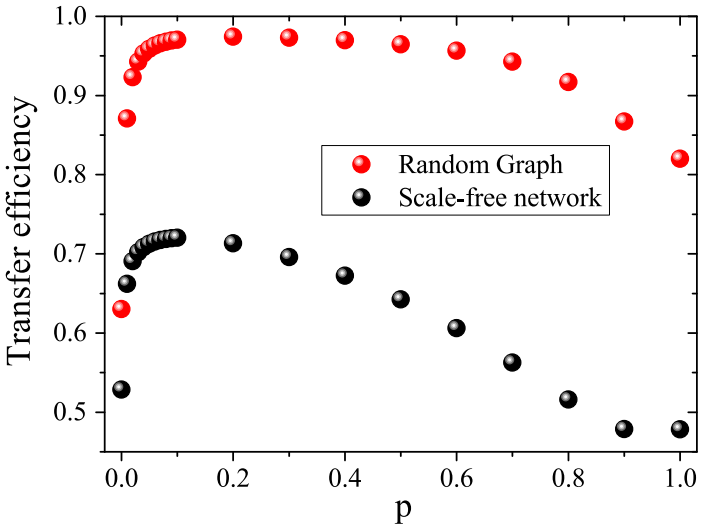

Figure 11. Transfer efficiency $\mathcal{E}(p)$ as a function of p for the cases of RG ($N = 200$) and SF networks ($N = 187$).

3.4. Other complex networks

Here we generalize the analysis above to a wider class of large complex networks. First of all, we find that, as expected, the transport efficiency $\mathcal{E}(p)$ of the CRW dynamics is almost linearly dependent on the graph diameter D introduced in section 2.1—see figure 12. In other words, the larger D is, the lower the transport efficiency $\mathcal{E}(p)$ on the corresponding network is. However, it turns out that the latter can be enhanced by adding some quantum coherence ($p < 1$) in the dynamics, as found above. Indeed, for a very large class of complex networks (including random graphs, small-worlds, scale-free networks, rings, stars, dendrimers, Kary trees, etc [1]), with $D > 3$, we find that the optimal transport efficiency is almost always achieved when

$$p_{opt} \sim 0.1. \tag{9}$$

The main exception is represented by FC graphs ($D = 1$) that are optimal for $p = 1$, i.e. for CRWs—see the inset of figure 12. This can be intuitively explained by the fact that for graphs with very small D (and so high mixing rate τ_{mix}), such as FC networks, CRWs propagate extremely quickly, while they are very slow for a linear chain (largest D, so smallest τ_{mix}). Vice versa, a basically opposite behavior is observed for QWs, i.e. larger D usually implies faster transport. The physical intuition behind this is that for large D one has a high number π of different eigenstates of the adjacency matrix A (since $\pi \geqslant D + 1$), and so less energy of trapped (or localized) states in the dynamics. This can be better understood by means of the notion of invariant subspaces introduced in [12]. The latter are defined as sets of eigenstates of the Hamiltonian that are orthogonal to the site connected to the sink, i.e. they are not affected by the open-system dynamics and their evolution is purely coherent and described by just a global phase. These invariant (trapped) states can be systematically found for any network with some degeneracy, as geometrical symmetries corresponding to large degenerate eigenspaces, and the more of them there are, the larger the amount of energy trapped in the system is. Hence, the FC

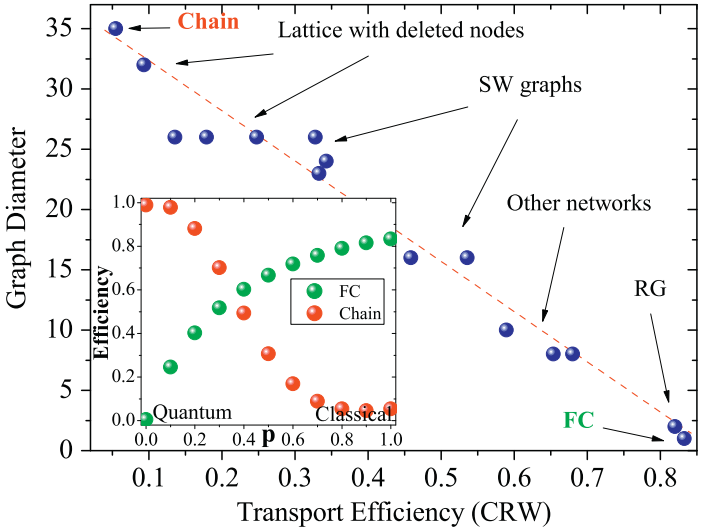

Figure 12. Graph diameter D as a function of the CRW transport efficiency $\mathcal{E}(p = 1, \bar{t})$ over different complex networks, with $\bar{t}$ being linearly proportional to the number of nodes N. The sites for the initial excitation and for the sink are randomly chosen. Inset: $\mathcal{E}(p)$ versus p for the extreme cases of linear chains and FC graphs.

graph ($D = 1$ and $\pi = 2$) is the worst geometry for QWs; indeed, because of destructive interference effects and the presence of an invariant subspace that is as large as possible, the transfer efficiency $\mathcal{E}(p = 0)$ cannot be larger than $1/(N - 1)$ [12]. However, by means of a universal mixing ($p \sim 0.1$) of, loosely speaking, 90% of QWs and 10% of CRWs, the invariant (trapped) subspaces are destroyed and the energy transport becomes optimal and robust, and, in particular, we find that this is irrespective of the particular underlying geometry of the complex network.

4. Conclusions and outlook

In this paper we extensively investigate the transport properties of quantum stochastic walks over a wide family of large complex networks. More specifically, we numerically calculate and compare the transport performances of these graphs through the transfer efficiency of a trapping site; this is also motivated by the structure of light-harvesting complexes, where the interplay of quantum coherence and environmental noise has recently been shown to play a fundamental role in explaining the remarkably efficient as well as fast exciton energy transfer. We find that, roughly speaking, the mixing of 90% of quantum dynamics and 10% of classical dynamics, i.e. for $p \sim 0.1$, leads to optimal transport efficiency. On top of that, this optimal behavior is not only relatively common on very different networks, but also robust with respect to geometric changes such as rewiring and deleting links.

However, there are some exceptions represented by very well-connected graphs (e.g., FCs and graphs with $D \propto N$), where, instead, classical random walks, i.e. $p = 1$ cases, provide the optimal transport into the trapping site. This might be a consequence of the fact that for such graphs there are many trapped states due to destructive interference (large invariant subspaces almost covering the full Hilbert space [12]), that are fully destroyed only at the classical limit.

The behavior for the transition from $p = 1$ to $p \sim 0.1$, when making the network less and less connected ($D \gg 1$), and a deeper analysis of this widespread and robust optimality, also based on a possible analytical derivation by means of Lieb–Robinson bounds [68, 69], will be investigated in a forthcoming paper.

Finally, our results could be tested through already experimentally available benchmark platforms such as cold atoms in optical lattices, artificial light-harvesting structures, and photonics-based architectures, and hence also may inspire the design of optimally efficient transport nanostructures for novel solar energy and quantum-information-based technologies.

Acknowledgments

This work was supported by EU FP7 Marie Curie Programme (Career Integration Grant) and by a MIUR–FIRB grant (project no. RBFR10M3SB). We acknowledge QSTAR for computational resources, based also on GPU-CUDA programming with NVIDIA Tesla C2075 GPU computing processors.

References

[1] Boccaletti S, Latora V, Moreno Y, Chavez M and Hwang D-U 2006 *Phys. Rep.* **424** 175
[2] Engel G S, Calhoun T R, Read E L, Ahn T-K, Mancal T, Cheng Y-C, Blankenship R E and Fleming G R 2007 *Nature* **446** 782
[3] Lee H, Cheng Y-C and Fleming G R 2007 *Science* **316** 1462
[4] Collini E, Wong C Y, Wilk K E, Curmi P M G, Brumer P and Scholes G D 2010 *Nature* **463** 644
[5] Panitchayangkoon G, Hayes D, Fransted K A, Caram J R, Harel E, Wen J, Blankenship R E and Engel G S 2010 *Proc. Natl Acad. Sci. USA* **107** 12766
[6] Hildner R, Brinks D, Nieder J B, Cogdell R J and van Hulst N F 2013 *Science* **340** 1448
[7] Mohseni M, Omar Y, Engel G S and Plenio M B (ed) 2013 *Quantum Effects in Biology* (Cambridge: Cambridge University Press)
[8] Huelga S F and Plenio M B 2013 *Contemp. Phys.* **54** 181–207
[9] Mohseni M, Rebentrost P, Lloyd S and Aspuru-Guzik A 2008 *J. Chem. Phys.* **129** 174106
[10] Plenio M B and Huelga S F 2008 *New J. Phys.* **10** 113019
[11] Olaya-Castro A, Lee C F, Fassioli Olsen F and Johnson N F 2008 *Phys. Rev.* B **78** 085115
[12] Caruso F, Chin A W, Datta A, Huelga S F and Plenio M B 2009 *J. Chem. Phys.* **131** 105106
Caruso F, Chin A W, Datta A, Huelga S F and Plenio M B 2010 *Phys. Rev.* A **81** 062346
[13] Chin A W, Datta A, Caruso F, Huelga S F and Plenio M B 2010 *New J. Phys.* **12** 065002
[14] Aharonov Y, Davidovich L and Zagury N 1993 *Phys. Rev.* A **48** 1687
[15] Mülken O and Blumen A 2011 *Phys. Rep.* **502** 37–87
[16] Santha M 2008 Quantum walk based search algorithms *Theory and Applications of Models of Computation* (*Lecture Notes in Computer Science* vol 4978) ed M Agrawal, D Z Du, Z H Duan and A S Li (Berlin: Springer) p 31
[17] Farhi E and Gutmann S 1998 *Phys. Rev.* A **58** 915–28
[18] Childs A, Farhi E and Gutmann S 2002 *Quantum Inf. Proc.* **1** 35
[19] Childs A 2009 *Phys. Rev. Lett.* **102** 180501
[20] Kempe J 2003 *Contemp. Phys.* **44** 307
[21] Kendon V 2007 *Math. Struct. Comp. Sci.* **17** 1169–220

[22] Venegas-Andraca S E 2012 *Quantum Inf. Process.* **11** 1015
[23] Ambainis A 2003 *Int. J. Quantum Inf.* **01** 507
[24] Grover L K 1997 *Phys. Rev. Lett.* **79** 325
[25] Childs A M, Gosset D and Webb Z 2013 *Science* **339** 791
[26] Bose S 2003 *Phys. Rev. Lett.* **91** 207901
[27] Christandl M, Datta N, Ekert A and Landahl A J 2004 *Phys. Rev. Lett.* **92** 187902
[28] Plenio M B, Hartley J and Eisert J 2004 *New. J. Phys.* **6** 36
[29] Caruso F, Huelga S F and Plenio M B 2010 *Phys. Rev. Lett.* **105** 190501
[30] Sánchez-Burillo E, Duch J, Gómez-Gardeñes J and Zueco D 2012 *Sci. Rep.* **2** 605
[31] Paparo G D and Martin-Delgado M A 2012 *Sci. Rep.* **2** 444
Paparo G D, Müller M, Comellas F and Martin-Delgado M A 2013 *Sci. Rep.* **3** 2773
[32] Garnerone S, Zanardi P and Lidar D 2012 *Phys. Rev. Lett.* **108** 230506
[33] Garnerone S 2012 *Phys. Rev.* A **86** 032342
[34] Strauch F W 2006 *Phys. Rev.* A **74** 030301(R)
[35] Du J, Li H, Xu X, Shi M, Wu J, Zhou X and Han R 2003 *Phys. Rev.* A **67** 042316
[36] Ryan C A, Laforest M, Boileau J C and Laflamme R 2005 *Phys. Rev.* A **72** 062317
[37] Schmitz H, Matjeschk R, Schneider C, Glueckert J, Enderlein M, Huber T and Schaetz T 2009 *Phys. Rev. Lett.* **103** 090504
[38] Zähringer F, Kirchmair G, Gerritsma R, Solano E, Blatt R and Roos C F 2010 *Phys. Rev. Lett.* **104** 100503
[39] Karski M, Frster L, Choi J-M, Steffen A, Alt W, Meschede D and Widera A 2009 *Science* **325** 174
[40] Perets H B *et al* 2008 *Phys. Rev. Lett.* **100** 170506
[41] Broome M A, Fedrizzi A, Lanyon B P, Kassal I, Aspuru-Guzik A and White A G 2010 *Phys. Rev. Lett.* **104** 153602
[42] Kitagawa T *et al* 2012 *Nat. Commun.* **3** 882
[43] Schreiber A, Cassemiro K N, Potocek V, Gabris A, Mosley P J, Andersson E, Jex I and Silberhorn C 2010 *Phys. Rev. Lett.* **104** 050502
[44] Schreiber A *et al* 2012 *Science* **336** 55–58
[45] Jeong Y-C, di Franco C, Lim H-T, Kim M and Kim Y-H 2013 *Nat. Commun.* **4** 2471
[46] Peruzzo A *et al* 2010 *Science* **329** 1500–3
[47] Owens J O *et al* 2011 *New J. Phys.* **13** 075003
[48] Sansoni L *et al* 2012 *Phys. Rev. Lett.* **108** 010502
[49] Rohde P P, Schreiber A, Stefanak M, Jex I and Silberhorn C 2011 *New J. Phys.* **13** 013001
[50] Avalle M and Serafini A 2013 arXiv:1311.0403
[51] Agliari E 2008 *J. Phys. A: Math. Theor.* **41** 445301
[52] Agliari E, Blumen A and Mülken O 2010 *Phys. Rev.* A **82** 012305
[53] Harel E 2012 *J. Chem. Phys.* **136** 174104
[54] Mohseni M, Shabani A, Lloyd S, Omar Y and Rabitz H 2013 *J. Chem. Phys.* **138** 204309
[55] Abasto D F, Mohseni M, Llloyd S and Zanardi P 2012 *Phil. Trans. R. Soc.* A **370** 3750–70
[56] Sarovar M and Whaley K B 2013 *New J. Phys.* **15** 013030
[57] van Mieghem P 2011 *Graph Spectra for Complex Networks* (Cambridge: Cambridge University Press)
[58] Whitfield J D, Rodríguez-Rosario C A and Aspuru-Guzik A 2010 *Phys. Rev.* A **81** 022323
[59] Watts D J and Strogatz S H 1998 *Nature* **393** 440
[60] Weiss G H 1994 *Aspects and Applications of the Random Walk* (Amsterdam: North-Holland)
[61] Kassal I and Aspuru-Guzik A 2012 *New J. Phys.* **14** 053041
[62] Watts D J and Strogatz S H 1998 *Nature* **393** 440
Watts D J 1999 *Small Worlds* (Princeton, NJ: Princeton University Press)
[63] Caruso F, Pluchino A, Latora V, Vinciguerra S and Rapisarda A 2007 *Phys. Rev.* E **75** 055101(R)
Caruso F, Latora V, Pluchino A, Rapisarda A and Tadić B 2006 *Eur. Phys. J.* B **50** 243–7
[64] Mülken O, Pernice V and Blumen A 2007 *Phys. Rev.* E **76** 051125

[65] Cao J and Silbey R J 2009 *J. Phys. Chem.* A **113** 13825–38
[66] Barabási A L and Albert R 1999 *Science* **286** 509
[67] Agliari E 2011 *Physica* A **390** 1853–60
[68] Kliesch M, Gogolin C and Eisert J 2013 Invited book chapter *Many-Electron Approaches in Physics, Chemistry and Mathematics: A Multidisciplinary View* ed L D Site and V Bach (Berlin: Springer) arXiv:1306.0716
[69] Kastoryano M J and Eisert J 2013 *J. Math. Phys* **54** 102201